VOL. 4, NO. 10, DECEMBER 2009 ISSN 1819-6608
ARPN Journal of Engineering and Applied Sciences


www.arpnjournals.com

INFLUENCE OF WALL PROPERTIES ON THE PERISTALTIC MOTION OF A HERSCHEL-BULKLEY FLUID IN A CHANNEL

G. C. Sankad and G. Radhakrishnamacharya
Department of Mathematics, National Institute of Technology, Warangal-506 004, India
E-Mail: grk.nitw@yahoo.com

ABSTRACT

Peristaltic motion of a Herschel-Bulkley fluid in a two-dimensional channel with wall effects is studied. Assuming that the wave length of the peristaltic wave is large in comparison to the mean half width of the channel, a perturbation method of solution is obtained in terms of wall slope parameter, under dynamic boundary conditions. Closed form expressions are derived for the stream function and average velocity and the effects of pertinent parameters on these flow variables have been studied. It has been observed that the time average velocity decreases with yield stress and power law index. Further, the time average velocity increases with rigidity in the wall. It has been observed that trapping occurs and the size of the trapped bolus increases with power-law index.

Keywords: peristaltic transport, herschel-bulkley fluid, yields stress, dynamic boundary conditions.

INTRODUCTION

Peristaltic motion is a form of fluid transport induced by a progressive wave of area contraction or expansion along the length of a distensible tube containing fluid. This kind of fluid transport occurs in many biological systems such as transport of urine through ureter, the swallowing process through the esophagus, food mixing and chyme movement in the intestine, blood flow in cardiac chambers etc. Also biomedical instruments such as heart lung machine use peristalsis to pump blood while mechanical devices like roller pumps use this mechanism to pump slurries and other corrosive fluids.

Significant initial investigations on mathematical models of peristalsis were done by Fung and Yih [1] and Shapiro *et al*., [2]. After these studies, several analytical, numerical and experimental attempts have been made to understand peristalsis in different situations for Newtonian and non-Newtonian fluids. Some of these studies have been done by Girija Devi and Devanathan [3], Radhakrishnamacharya [4], Misery *et al*., [5], Mishra and Rao [6], Srinivasacharya *et al*., [7], Hayat *et al*., [8], Kothandapani and Srinivas [9] and Sobh [10].

Though the Newtonian and several non-Newtonian models have been used to study the motion of blood, it is realized (Blair and Spanner, [11]) that Herschel-Bulkley model describes the behavior of blood very closely.

Herschel-Bulkley fluids are a class of non-Newtonian fluids that require a finite stress, known as yield stress, in order to deform. Therefore, these materials behave like rigid solids when the local shear is below the yield stress. Once the yield stress is exceeded, the material flows with a non-linear stress-strain relationship either as a shear-thickening fluid, or a shear-thinning one. Few examples of fluids behaving in this manner include paints, food products, plastics, slurries, pharmaceutical products etc.

Vajravelu *et al*., [12] considered peristaltic pumping of a Herschel-Bulkley fluid in a channel. Maruthi Prasad and Radhakrishnamacharya [13] discussed peristaltic transport of a Herschel-Bulkley fluid in a channel in the presence of magnetic field of low intensity. Recently Amit Medhavi [14] studied peristaltic pumping of a Herschel-Bulkley fluid under long wavelength and low Reynolds number approximation.

However, the interaction of peristalsis with elastic properties of the wall has not received much attention. Mittra and Prasad [15] studied peristaltic transport in a two-dimensional channel considering the elasticity of the walls under the approximation of small amplitude ratio with dynamic boundary conditions. Srinivasulu and Radhakrishnamacharya [16] studied the same problem under long wavelength approximation. Muthu *et al*., [17] extended the analysis of Mittra and Prasad [15] to micropolar fluids.

Hence, a mathematical model is presented in this paper to investigate the influence of wall effects on the peristaltic motion of a Herschel-Bulkley fluid in a two-dimensional channel using the dynamic boundary conditions. A perturbation method of solution has been obtained in terms of wall slope parameter assuming that the wave length of the peristaltic wave is large in comparison to the mean half width of the channel. Closed form expressions for the stream function and average velocity have been derived and the effects of various parameters on these flow variables have been studied.

FORMULATION AND SOLUTION OF THE PROBLEM

Consider the flow of Herschel-Bulkley fluid through a two dimensional channel of uniform cross section with flexible walls on which are imposed traveling sinusoidal waves of long wave length. A cartesian coordinate system (x, y) is chosen with x-axis aligned with the central line of the channel and in the direction of propagation of waves. The traveling waves are represented

$$\eta(x,t) = d + a\sin\frac{2\pi}{\lambda}(x - ct), \qquad (1)$$

Where d is the mean half width of the channel, t is the time, a is the amplitude, λ is the wave length and c is the speed of the traveling waves (Figure-1).

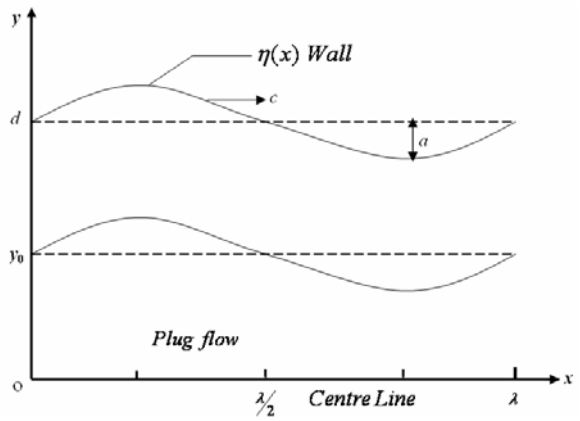

Figure-1. Geometry of the problem.

The governing equation of the motion of the flexible wall may be expressed as

$$L(\eta) = p - p_0 \tag{2}$$

where L is the operator, which is used to represent the motion of stretched membrane with damping forces such that

$$L = -T\frac{\partial^2}{\partial x^2} + m\frac{\partial^2}{\partial t^2} + C\frac{\partial}{\partial t}. \tag{3}$$

Here T is the tension in the membrane, m is the mass per unit area and C is the coefficient of the viscous damping force.

It is assumed that $p_0 = 0$ and the channel walls are inextensible so that only their lateral motions normal to the unreformed positions occur. Thus, the horizontal displacement is assumed to be zero.

The equations governing the flow of Herschel-Bulkley fluid for the present problem, under long wavelength approximation and neglecting inertia terms, are (Vajravelu *et al*., [12], Maruthi Prasad and Radhakrishnamacharya [13])

$$\frac{\partial}{\partial y}\left(\tau_{yx}\right) = -\frac{\partial p}{\partial x}, \tag{4}$$

Where τ_{yx} for the Herschel-Bulkley fluid is given by

$$\left(-\frac{\partial u}{\partial y}\right)^n = \frac{1}{\mu}\left(\tau_{yx} - \tau_0\right), \qquad \tau_{yx} \geq \tau_0 \tag{5}$$

$$\frac{\partial u}{\partial y} = f(\tau) = 0, \qquad \tau_{yx} \leq \tau_0 \tag{6}$$

Where p is the pressure, μ and ($n \geq 1$) are consistency and flow behavior indexes, respectively and representing the non-Newtonian effects.

Relation (6) corresponds to the vanishing of the velocity gradient in the region in which $\tau_{yx} \leq \tau_0$ and implies a plug flow, when shear stress in the fluid is very high (i.e. $\tau_{yx} \geq \tau_0$), the power law behavior is indicated. It is noted that above Herschel-Bulkley fluid model reduces to Bingham fluid when n=1; to power law fluid when $\tau_0 = 0$ and to Newtonian fluid when n=1 and $\tau_0 = 0$. It is important to mention that the plug core width increases with yield stress τ_0 and also with the flow behavior index n.

The corresponding boundary conditions are

$$u = 0 \text{ at } \quad y = \eta, \tag{7}$$

$$\frac{\partial u}{\partial y} = 0 \text{ and } \tau_{yx} = 0 \quad \text{at} \quad y = 0. \tag{8}$$

The dynamic boundary conditions at the flexible walls, following Mittra and Prasad [15] can be written as

$$\frac{\partial p}{\partial x} = \frac{\partial}{\partial x}L(\eta) = -T\frac{\partial^3 \eta}{\partial x^3} + m\frac{\partial^3 \eta}{\partial t^2 \partial x} + C\frac{\partial^2 \eta}{\partial t \partial x}. \tag{9}$$

Further, defining the stream function ψ by

$$u = \frac{\partial \psi}{\partial y} \quad \text{and} \quad v = -\frac{\partial \psi}{\partial x}, \tag{10}$$

and the following non dimensional quantities

$$\left.\begin{aligned} x' &= \frac{x}{\lambda},\ y' = \frac{y}{d},\ u' = \frac{u}{c},\ t' = \frac{ct}{\lambda},\ \tau_0' = \frac{\tau_0}{\mu\left(c/d\right)^n},\ \tau_{yx}' = \frac{\tau_{yx}}{\mu\left(c/d\right)^n}, \\ \eta' &= \frac{\eta}{d},\ p' = \frac{pd^{n+1}}{\lambda \mu c^n},\ \psi' = \frac{\psi}{cd} \end{aligned}\right\} \tag{11}$$

equations (4 - 9), after dropping the primes, can be written as

$$\frac{\partial}{\partial y}\left(\tau_{yx}\right) = -\frac{\partial p}{\partial x} \text{ where } \tau_{yx} = \left(-\frac{\partial u}{\partial x}\right)^n + \tau_0, \quad \tau_{yx} \geq \tau_0, \tag{12}$$

$$\left(\frac{\partial u}{\partial y}\right) = 0, \quad \tau_{yx} \leq \tau_0 \tag{13}$$

where τ_{yx} and τ_0 are dimensionless shearing and yield stress respectively.

The boundary conditions are

$$\psi = 0; \quad \psi_{yy} = 0 \quad \text{at} \quad y = 0, \tag{14}$$

$$\left.\begin{aligned}\psi_y = 0 \quad at \quad y = \eta = 1 + \varepsilon \sin 2\pi(x-t),\\ \tau_{yx} = 0 \quad at \quad y = 0,\end{aligned}\right\} \tag{15}$$

$$\frac{\partial p}{\partial x} = -\varepsilon\left[(2\pi)^3 \cos 2\pi(x-t)(E_1+E_2) - (2\pi)^2 E_3 \sin 2\pi(x-t)\right] \tag{16}$$

Where $\varepsilon\left(=a/d\right)$ is the amplitude ratio,

$$E_1 = -\frac{Td^{n+2}}{\lambda^3 \mu c^n},\ E_2 = \frac{md^{n+2}}{\lambda^3 \mu c^{n-2}}\ and\ E_3 = \frac{Cd^{n+2}}{\lambda^2 \mu c^{n-1}}$$

are the non-dimensional elasticity parameters.

The non-dimensional quantities E_1, E_2 and E_3 are related to the wall motion through the dynamic boundary condition (16). The parameters E_1 and E_2 respectively represent the rigidity and stiffness of the wall. The viscous damping force in the wall is represented by E_3. In particular, E_3=0 implies that the walls move up and down with no damping force on them and hence indicates the case of elastic walls (i.e. E_3=0).

Solving Equation (12) subject to the boundary conditions (14)-(16), we obtain the expression for velocity as

$$u = \frac{1}{P(k+1)}\left[(P\eta - \tau_0)^{k+1} - (Py - \tau_0)^{k+1}\right], \tag{17}$$

where $\mathrm{P} = -\frac{\partial \mathrm{p}}{\partial \mathrm{x}}$ *and* $k = \frac{1}{n}$.

We find the upper limit of the plug flow region by using the boundary condition that $\psi_{yy} = 0 \ at \ y = y_0$ so that $y_0 = \frac{\tau_0}{P}$.

Also, by using the condition $\tau_{yx} = \tau_\eta \ at \ y = \eta$, we obtain $P = \frac{\tau_0}{\eta}$.

Hence

$$\frac{y_0}{\eta} = \frac{\tau_0}{\tau_\eta}, \qquad 0 < \tau < 1. \tag{18}$$

The expression for the fluid velocity in the plug flow, u_p, region is obtained by substituting $y = y_0$ in equation (17) and this obviously satisfies equation (13) in the plug flow region.

Hence, we get

$$u_p = \frac{1}{P(k+1)}\left[(P\eta - \tau_0)^{k+1}\right], \tag{19}$$

Integrating equations (17) and (19) and using the conditions $\psi_p = 0$ at $y = 0$ and $\psi = \psi_p$ at $y = y_0$, we obtain the stream function as

$$\psi_c = \frac{P^k}{k+1}\left[y(\eta - y_0)^{k+1} - \frac{1}{k+2}(y - y_0)^{k+2}\right] \quad \text{for} \quad y_0 \le y \le \eta \tag{20}$$

and

$$\psi_p = \frac{P^k}{k+1} y(\eta - y_0)^{k+1} \quad \text{for} \quad 0 \le y \le y_0. \tag{21}$$

Averaging equations (17) and (19) over one period of the motion yields the average velocity $\bar{u}$ as

$$\bar{u} = \int_0^1 u\, dt \tag{22}$$

It can be noticed that when the yield stress $\tau_0 = 0$ and power-law index n =1, i.e., when fluid becomes Newtonian, the expressions for $\bar{u}$ and ψ reduce to the corresponding expressions for Newtonian fluid as given by Srinivasulu and Radhakrishnamacharya (Srinivasulu and Radhakrishnamacharya [16]).

RESULTS AND DISCUSSIONS

In this study, the effects of wall parameters, yield stress and power-law index on the peristaltic motion of a Herschel-Bulkley fluid are investigated. In order to discuss the effects of various parameters on the flow variables, the time average velocity $\bar{u}$ has been calculated for various values of these parameters. Mathematica software has been used for the numerical evaluation of the analytical results and some important results are graphically presented in Figures 2 to 17.

The average velocity for the present problem depends upon the following important non-dimensional quantities.

a) E_1, E_2 and E_3, the wall parameters which characterize the viscoelastic behavior of the flexible walls.
b) The power-law index n determines the non-linear behavior of the fluid, for n<1, it describes shear thinning behavior and for n>1, shear thickening.
c) The yield stress τ_0.

The effect of the rigidity parameter for the membrane E_1 on the time average velocity $\bar{u}$ for the case of no stiffness ($E_2 = 0$) and no viscous damping in the channel wall ($E_3 = 0$) is shown in Figures 2 and 3. It is seen that the time average velocity $\bar{u}$ increases with rigidity (E_1) but decreases with power-law index n.

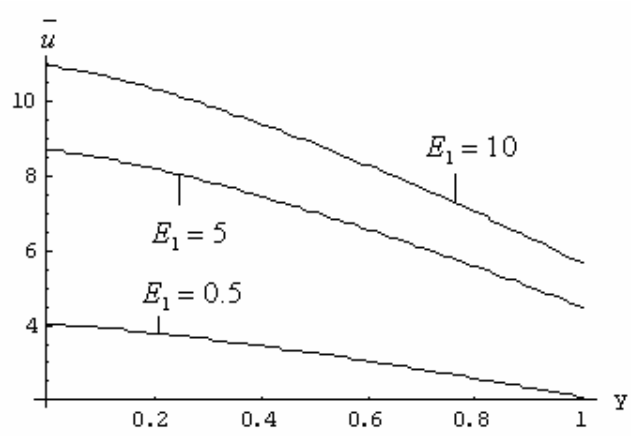

Figure-2. Effect of E_1 on average velocity $\bar{u}$ (ε =0.6, E_2=0, E_3=0.0, n=3, τ_0 =0.2).

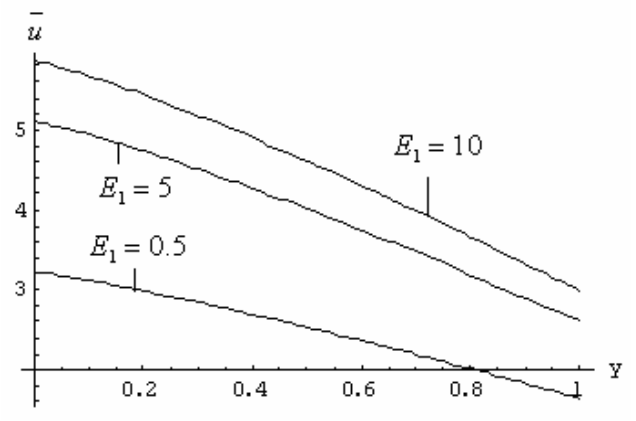

Figure-3. Effect of E_1 on average velocity $\bar{u}$ (ε =0.6, E_2=0, E_3=0.0, n=5, τ_0 =0.2).

Figures 4 to 6 show that the time average velocity $\bar{u}$ increases with the rigidity of the membrane (E_1) with stiffness ($E_2 \neq 0$) and without stiffness ($E_2 = 0$) in the channel wall and also in the presence ($E_3 \neq 0$) and absence ($E_3 = 0$) of the dissipative effects.

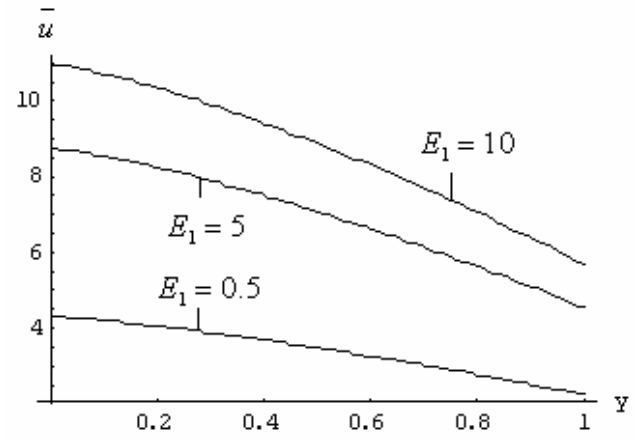

Figure-4. Effect of E_1 on average velocity $\bar{u}$ (ε =0.6, E_2=0.1, E_3=0.0, n=3, τ_0 =0.2).

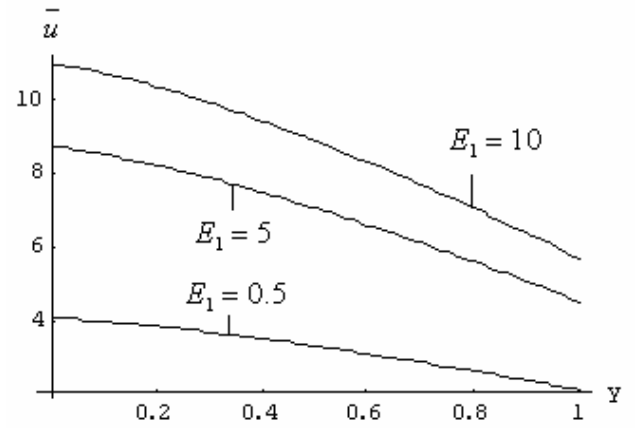

Figure-5. Effect of E_1 on average velocity $\bar{u}$ (ε =0.6, E_2=0, E_3=0.1, n=3, τ_0 =0.2).

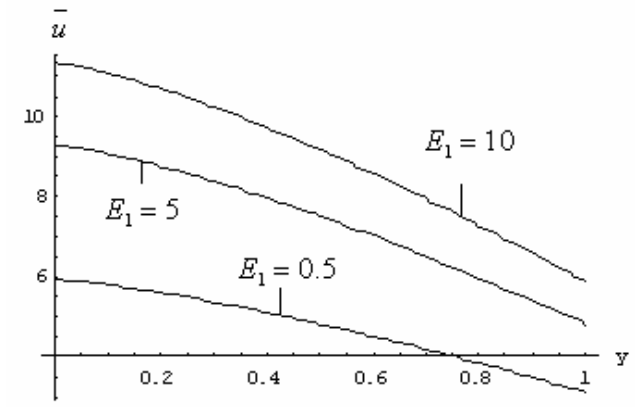

Figure-6. Effect of E_1 on average velocity $\bar{u}$ (ε =0.2, E_2=1, E_3=0.9, n=3, τ_0 =0.2).

It can be observed that the time average velocity $\bar{u}$ increases with stiffness in the wall (E_2) [Figures 7 and 8] and viscous damping force (E_3) [Figures 9 and 10].

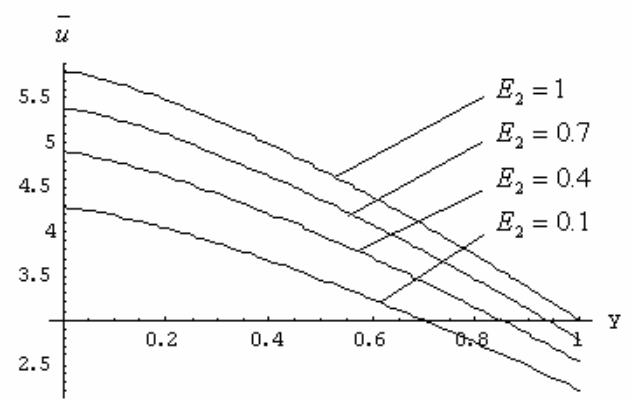

Figure-7. Effect of E_2 on average velocity $\bar{u}$ (ε=0.6, E_1= 0.5, E_3=0.0, n=3, τ_0 =0.2).

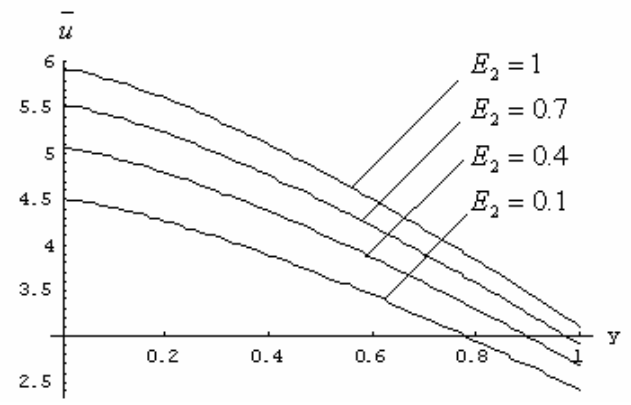

Figure-8. Effect of E_2 on average velocity $\bar{u}$ (ε=0.6, E_1= 0.5, E_3=0.9, n=3, τ_0 =0.2).

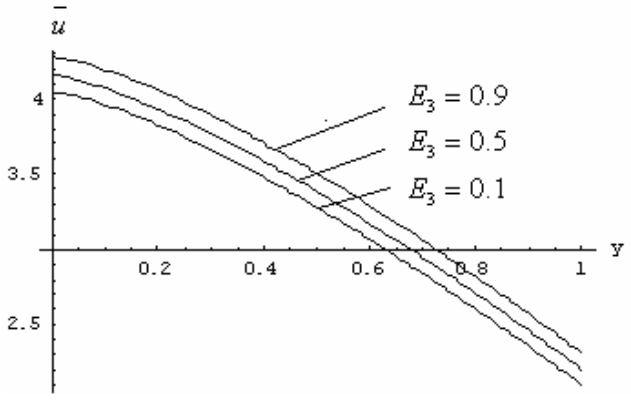

Figure 9. Effect of E_3 on average velocity $\bar{u}$ (ε=0.6, E_1= 0.5, E_2=0.0, n=3, τ_0 =0.2).

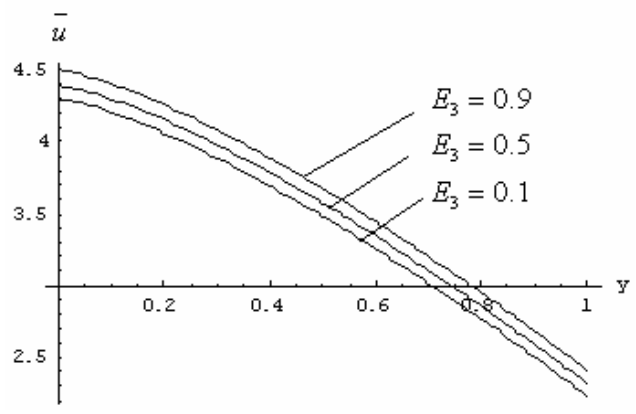

Figure-10. Effect of E_3 on average velocity $\bar{u}$ (ε=0.6, E_1= 0.5, E_2=0.1, n=3, τ_0 =0.2).

The effect of the power-law index n on the time average velocity $\bar{u}$ is shown in Figures 11 to 13. It is observed that the time average velocity decreases with power-law index n in the presence and absence of stiffness as well as dissipative effects in the wall.

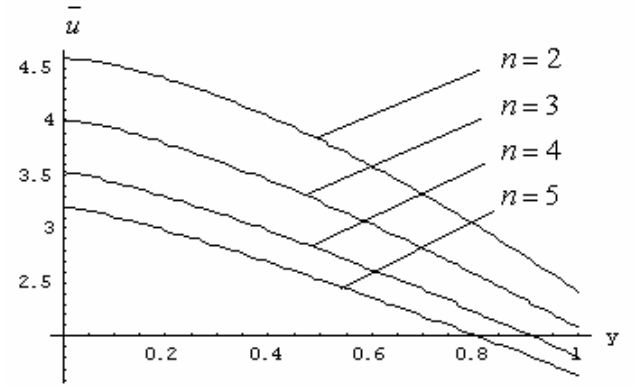

Figure-11. Effect of n on average velocity $\bar{u}$ (ε=0.6, E_1= 0.5, E_2=0.0, E_3=0.0, τ_0 =0.2).

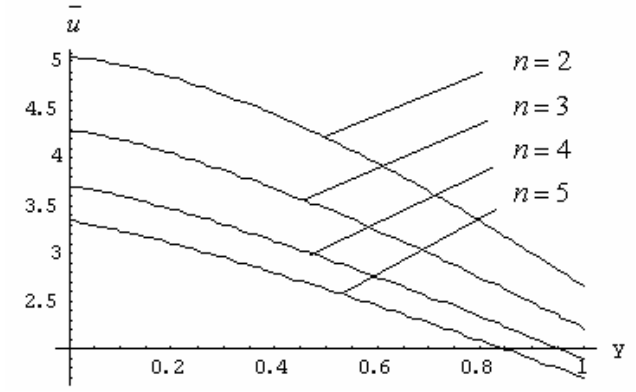

Figure-12. Effect of n on average velocity $\bar{u}$ (ε=0.6, E_1= 0.5, E_2=0.1, E_3=0.0, τ_0 =0.2).

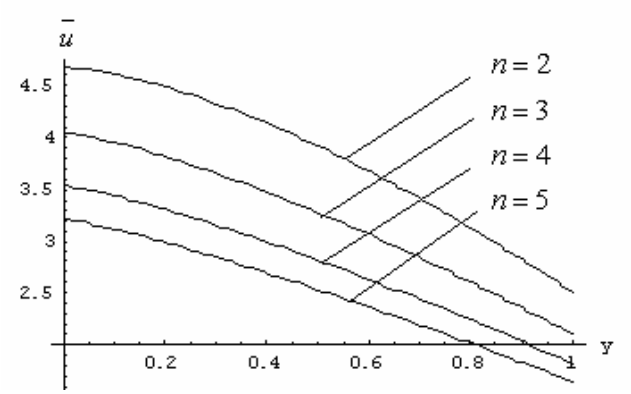

Figure-13. Effect of *n* on average velocity $\bar{u}$ (ε=0.6, E_1= 0.5, E_2=0.0, E_3=0.1, τ_0 =0.2).

Figures 14 to 17 show the effects of yield stress τ_0 on the time average velocity $\bar{u}$. It can be observed from Figures 14 and 15 that for the case of shear thinning (n<1), the time average velocity decreases with yield stress. Further, flow reversal takes place when there is no viscous damping force in the channel wall ($E_3 = 0$) [Figure-14]. Also, the time average velocity $\bar{u}$ decreases as yield stress τ_0 increases when there is stiffness ($E_2 \neq 0$) and viscous damping force ($E_3 \neq 0$) in the wall for the case of shear thickening (n>1) [Figures 16 and 17].

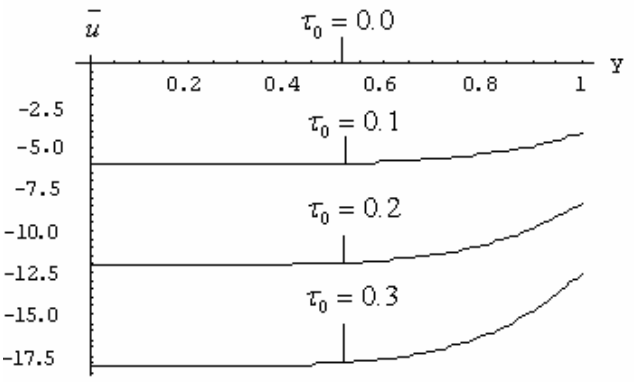

Figure-14. Effect of τ_0 on average velocity $\bar{u}$ (ε=0.6, E_1= 0.5, E_2=0.1, E_3=0.0, n=0.2).

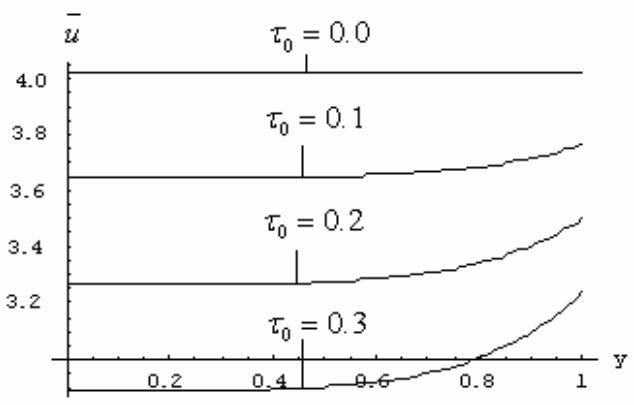

Figure-15. Effect of τ_0 on average velocity $\bar{u}$ (ε=0.6, E_1= 0.5, E_2=0.0, E_3=0.1, n=0.2).

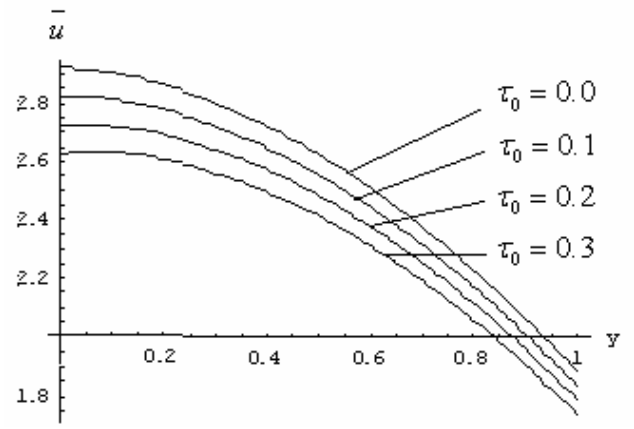

Figure16. Effect of τ_0 on average velocity $\bar{u}$ (ε=0.6, E_1= 0.5, E_2=0.1, E_3=0.1, n=1.2).

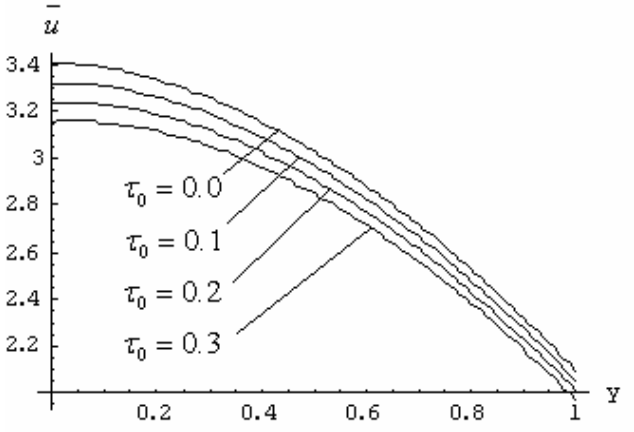

Figure-17. Effect of τ_0 on average velocity $\bar{u}$ (ε=0.6, E_1= 0.5, E_2=1, E_3=0.1, n=1.25).

The effect of various parameters on stream line pattern is shown in Figures 18 to 22. It is interesting to note that trapping, an important feature of peristalsis, is

observed in all the cases. It may be noted that trapping was observed by Vajravelu *et al*. (2005) also.

Figure-18 shows that for higher rigidity (E_1), the stream lines get closer and the size of the trapped bolus increases in some region. Also, as the stiffness in the wall (E_2) and viscous damping (E_3) increases, the size of the trapped bolus increases [Figures 19 and 20].

It can be seen from Figures 21 and 22 that the size of the trapped bolus increases with the power-law index n but there is no effect of yield stress τ_0 on the stream line pattern.

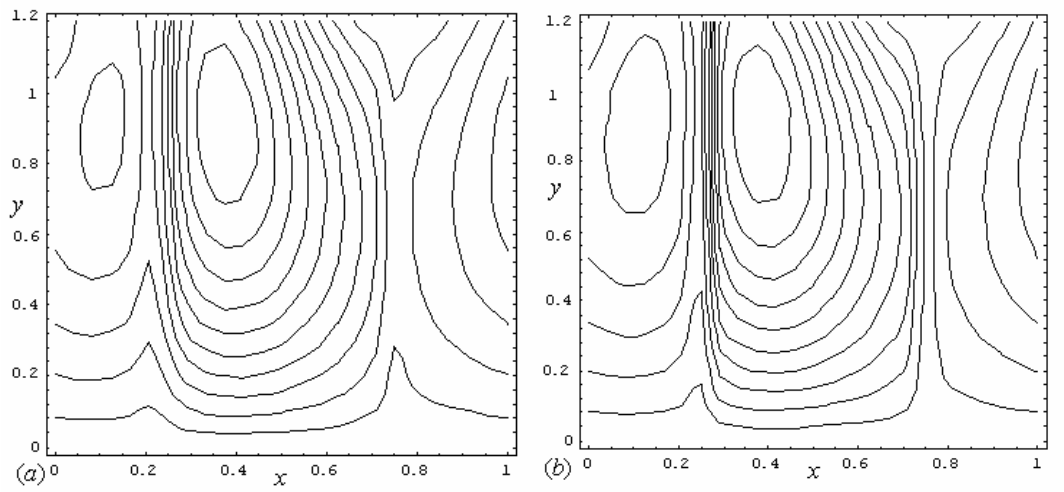

Figure-18. Effect of E_1 on stream line pattern of Herschel-Bulkley fluid a) (ε =0.2, E_1=0.5, E_2=0.4, E_3=0.5, n=3, τ_0 =0.2) b) (ε =0.2, E_1=10, E_2=0.4, E_3=0.5, n=3, τ_0 =0.2).

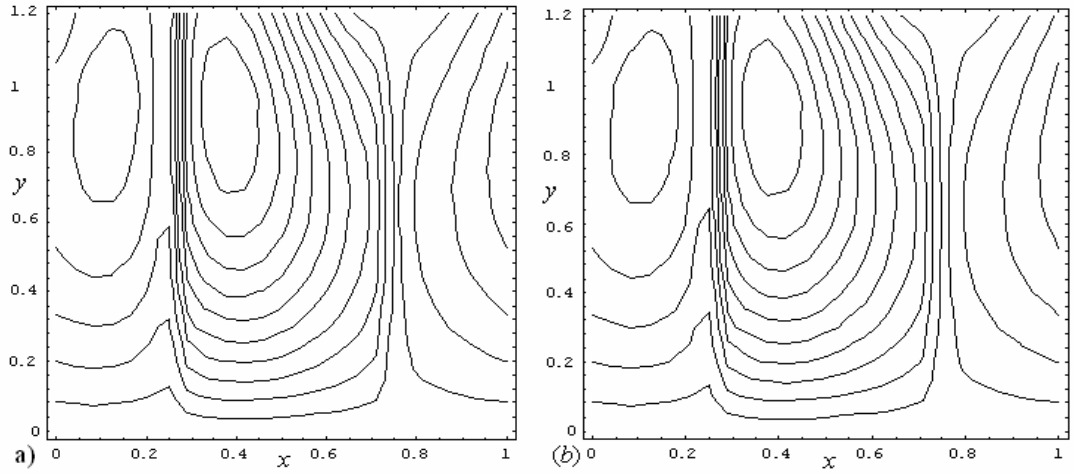

Figure-19. Effect of E_2 on stream line pattern of Herschel-Bulkley fluid a) (ε =0.2, E_1=5, E_2=0.1, E_3=0.5, n=3, τ_0 =0.2) b) (ε =0.2, E_1=5, E_2=1, E_3=0.5, n=3, τ_0 =0.2).

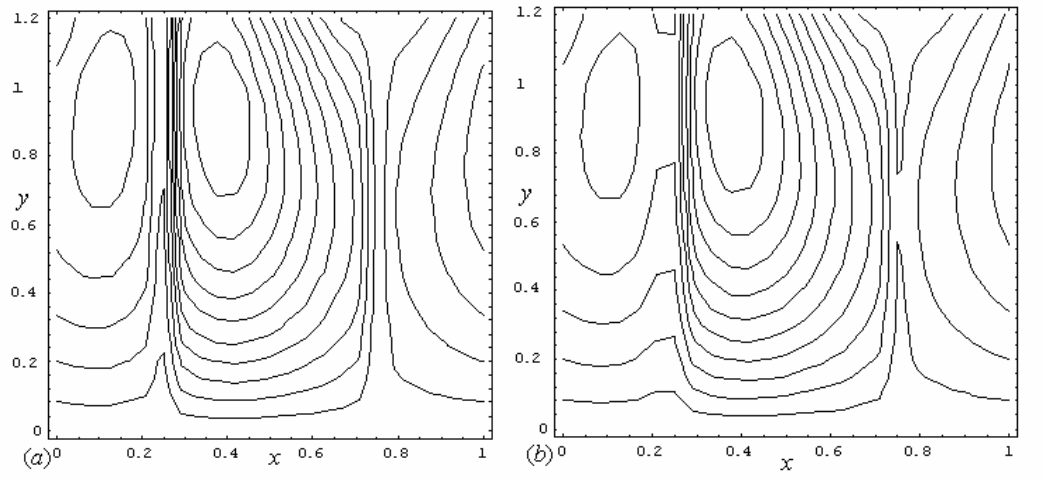

Figure-20. Effect of E_3 on stream line pattern of Herschel-Bulkley fluid a) (ε =0.2, E_1=5, E_2=0.4, E_3=0.1, n=3, τ_0 =0.2) b) (ε =0.2, E_1=5, E_2=0.4, E_3=0.9, n=3, τ_0 =0.2).

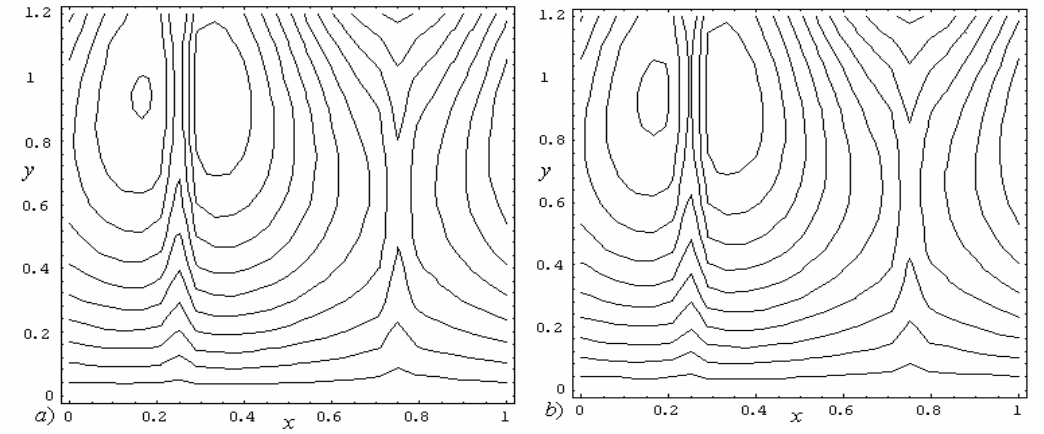

Figure-21. Effect of n on stream line pattern of Herschel-Bulkley fluid a) (ε =0.2, E_1=5, E_2=0.4, E_3=0.5, n=9, τ_0 =0.2) b) (ε =0.2, E_1=5, E_2=0.4, E_3=0.5, n=10, τ_0 =0.2).

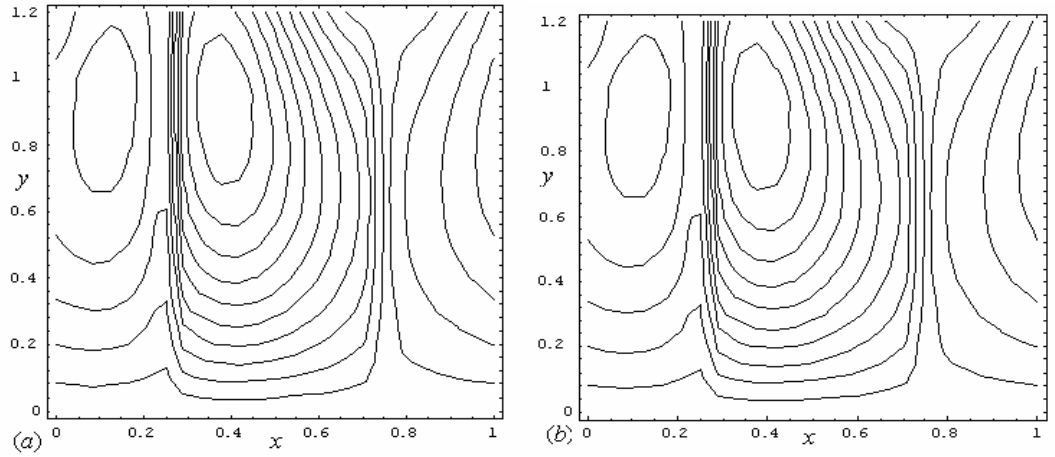

Figure-22. Effect of τ_0 on stream line pattern of Herschel-Bulkley fluid a) (ε =0.2, E_1=5, E_2=0.4, E_3=0.5, n=3, τ_0 =0.1) b) (ε =0.2, E_1=5, E_2=0.4, E_3=0.5, n=3, τ_0 =0.3).

CONCLUSIONS

We have analyzed the problem of the peristaltic motion of a Herschel-Bulkley fluid in a two-dimensional channel under the influence of wall properties. The governing equations have been linearized under long wavelength approximation and analytical expressions for time average velocity and stream function have been derived. The effects of various parameters on time average velocity and stream line pattern have been studied. It is found that the time average velocity increases with rigidity, stiffness and dissipative nature of the walls but decreases with power-law index and yield stress. Stream line pattern shows that the size of the trapped bolus increases in some region with higher rigidity in the wall.

REFERENCES

[1] Fung Y.C. and Yih C.S. 1968. Peristaltic transport. J. Appl. Mech. Trans. ASME. 35: 669-675.

[2] Shapiro A.H., Jaffrin M.Y. and Weinberg S.L. 1969. Peristaltic Pumping with long wavelengths at low Reynolds number. J. Fluid Mech. 37: 799-825.

[3] Girija Devi R. and Devanathan R. 1975. Peristaltic motion of micropolar fluid. Proc. Indian Acad. Sci. 81: 149-163.

[4] Radhakrishnamacharya G. 1982. Long wave length approximation to peristaltic motion of power law fluid. Rheol. Acta. 21: 30-35.

[5] Misery A.M.EL., Shehawey E.F.EL. And Hakeem A. 1996. Peristaltic motion of an incompressible generalized Newtonian fluid in a planar channel. J. Phys. Soc. Japan. 65(11): 3524-3529.

[6] Mishra M. and Rao A.R. 2003. Peristaltic transport of a Newtonian fluid in an asymmetric channel. Z Angew math. Phy. 54: 532-550.

[7] Srinivasacharya D., Mishra M. and Rao A.R. 2003. Peristaltic pumping of a micropolar fluid in a tube. Acta Mech.161: 165-178.

[8] Hayat T., Wang Y., Hutter K., Asghar S. and Siddiqui A.M. 2004. Peristaltic transport of an Oldroyd-B fluid in a planner channel. Math. Problems Eng. 4: 347-376.

[9] Kothandapani M. and Srinivas S. 2008. On the influence of wall properties in the MHD peristaltic transport with heat transfer and porous medium. Phys. Lett. A372: 4586-4591.

[10] Sobh A.M. 2008. Interaction of Couple stresses and slip flow on peristaltic transport in uniform and non-uniform channels. Turkish J. Eng. Env. Sci. 32: 117-123.

[11] Blair G.W.S. And Spanner D.C. 1974. An Introduction to Bioreheology. Elsevier, Amsterdam.

[12] Vajravelu K., Sreenadh S. And Ramesh Babu V. 2005. Peristaltic pumping of a Herschel-Bulkley fluid in a channel. Appl. Math. Comput. 169: 726-735.

[13] Maruthi Prasad K. and Radhakrishnamacharya G. 2007. Peristaltic transport of a Herschel-Bulkley fluid in a channel in the presence of Magnetic field of low Intensity. Int. J. Computational Intelligence Research and Applications. 1: 71-81.

[14] Medhavi Amit. 2008. Peristaltic pumping of a non-Newtonian fluid. AAM. 3(1): 137-148.

[15] Mittra T.K. And Prasad S.N. 1973. On the influence of wall properties and Poiseuille flow in peristalsis. J. Biomech. 6: 681-693.

[16] Radhakrishnamacharya G. and Srinivasulu Ch. 1999. Effect of elasticity of wall on peristaltic transport. Proceedings of ISTAM (India). 50-59.

[17] Muthu P., Rathish Kumar B.V. and Chandra P. 2003. On the influence of wall properties in the peristaltic motion of micropolar fluid. ANZIAM J. 45: 245-260.